

Accepted Manuscript

Discovery and optimization of phthalazinone derivatives as a new class of potent dengue virus inhibitors

Dong Lu, Jianan Liu, Yunzhe Zhang, Feifei Liu, Limin Zeng, Runze Peng, Li Yang, Huazhou Ying, Wei Tang, Wuhong Chen, Jianping Zuo, Xiankun Tong, Tao Liu, Youhong Hu

PII: S0223-5234(18)30008-4

DOI: [10.1016/j.ejmech.2018.01.008](https://doi.org/10.1016/j.ejmech.2018.01.008)

Reference: EJMECH 10085

To appear in: *European Journal of Medicinal Chemistry*

Received Date: 12 October 2017

Revised Date: 2 January 2018

Accepted Date: 4 January 2018

Please cite this article as: D. Lu, J. Liu, Y. Zhang, F. Liu, L. Zeng, R. Peng, L. Yang, H. Ying, W. Tang, W. Chen, J. Zuo, X. Tong, T. Liu, Y. Hu, Discovery and optimization of phthalazinone derivatives as a new class of potent dengue virus inhibitors, *European Journal of Medicinal Chemistry* (2018), doi: 10.1016/j.ejmech.2018.01.008.

This is a PDF file of an unedited manuscript that has been accepted for publication. As a service to our customers we are providing this early version of the manuscript. The manuscript will undergo copyediting, typesetting, and review of the resulting proof before it is published in its final form. Please note that during the production process errors may be discovered which could affect the content, and all legal disclaimers that apply to the journal pertain.

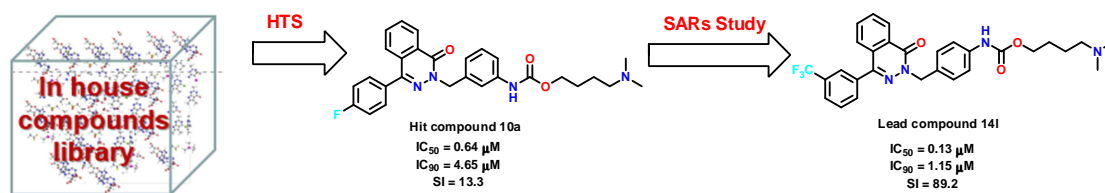


Title:

Discovery and optimization of phthalazinone derivatives as a new class of potent dengue virus inhibitors

ACCEPTED MANUSCRIPT

Graphical abstract



A series of novel phthalazinone derivatives was synthesized and evaluated for their *in vitro* anti-DENV-2 activities. The SAR study led to the discovery of the most promising compound **14I**.

Highlights

- Novel phthalazinones as dengue virus inhibitors were synthesized and evaluated.
- The SAR of the phthalazinones for anti-dengue virus activity was explored.
- Lead compound **14i** with acceptable pharmacokinetics profiles was investigated.
- The computerized docking study of **14i** with dengue NS3 protease was performed.

Title:

Discovery and Optimization of Phthalazinone derivatives as a New Class of Potent Dengue Virus Inhibitors

Dong Lu^{†,b,c}, Jianan Liu^{†,b,c}, Yunzhe Zhang^{†,a}, Feifei Liu^{b,c}, Limin Zeng^b, Runze Peng^{b,c}, Li Yang^b, Huazhou Ying^a, Wei Tang^b, Wuhong Chen^b, Jianping Zuo^b, Xiankun Tong^{*,b}, Tao Liu^{*,a}, Youhong Hu^{*,a,b}

^aZhejiang Province Key Laboratory of Anti-Cancer Drug Research, College of Pharmaceutical Sciences, Zhejiang University, Hangzhou 310058, China

^bState Key Laboratory of Drug Research, Shanghai Institute of Materia Medica, Chinese Academy of Sciences, 555 Zu Chong Zhi Road, Shanghai 201203, China

^cUniversity of Chinese Academy of Sciences, No.19A Yuquan Road, Beijing 100049, China

*Corresponding author: E-mail: yhhu@simm.ac.cn, Lt601@zju.edu.cn, xktong@simm.ac.cn

DL, JL and YZ equally contributed to this work.

Abstract:

Using a dengue replicon cell line-based screening, we identified 3-(dimethylamino)propyl(3-((4-(4-fluorophenyl)-1-oxophthalazin-2(1H)-yl)methyl)phenyl)carbamate (**10a**) as a potent DENV-2 inhibitor, with an IC₅₀ value of 0.64 μM. A series of novel phthalazinone derivatives based on hit **10a** were synthesized and evaluated for their *in vitro* anti-DENV activity and cytotoxicity. The subsequent SAR study and optimization led to the discovery of the most promising compound **14l**, which displayed potent anti-DENV-2 activity, with low IC₅₀ value against DENV-2 RNA replication of 0.13 μM and high selectivity (SI = 89.2) with acceptable pharmacokinetics profiles.

Key words: Phthalazinone; Dengue Virus; Inhibitor; Optimization; SAR

1. Introduction

Dengue Virus (DENV) belongs to the genus *Flavivirus*, family *Flaviviridae*, which includes *Flavivirus*, *Pestivirus*, and *Hepacivirus*. The genome of Dengue Virus is a positive-sense, single-stranded RNA of approximately 11 kb, encoding three structural proteins (capsid, premembrane and envelope) and seven non-structural proteins (NS1, NS2A, NS2B, NS3, NS4A, NS4B and NS5). Dengue Virus contains four serotypes, known as DENV-1-4[1-4].

Dengue, generally transmitted by *Aedes* mosquitoes, remains a major public health issue in tropical and subtropical areas, which is strongly associated with flu-like symptoms, life-threatening dengue hemorrhagic fever (DHF) and dengue shock syndrome (DSS)[5-7]. Indeed, one recent estimate indicates 390 million dengue infections per year, of which about 96 million develop symptoms[8]. The incidence of dengue has grown dramatically around the world in recent years[8].

Currently, there is still no drugs available for the treatment of DENV. Indeed, the treatment of dengue infections is confined to symptomatic alleviation and supportive care. Thus, the development of effective and safe anti-DENV therapeutics remains of utmost importance. With the understanding of the dengue pathogenesis, in the recent years, a number of anti-DENV agents

targeting both dengue viral and host proteins have been discovered, including entry inhibitors, capsid inhibitors, NS4B inhibitors and protease inhibitors[9-20]. Among them, Celgosivir, is under clinical trial currently. Dengue vaccine developed by Sanofi Pasteur has been listed in more than 10 countries including United States, India, Australia, Mexico and Brazil to prevent dengue fever[21].

Figure 1

High-throughput phenotypic screening is a powerful tool to identify compounds that targeting either viral proteins and/or host proteins, which are essential for viral replication. As a result of DENV-2 screening of our in-house collection of compounds, a novel chemical compound 3-(dimethylamino)propyl(3-((4-(4-fluorophenyl)-1-oxophthalazin-2(1H)-yl)methyl)phenyl)carbamate (**10a**, Figure 2) was identified as a potent DENV inhibitor, with an IC_{50} value of 0.64 μ M against DENV-2 RNA replication *in vitro*. In consideration of its novel structural scaffold, differing from those of all reported DENV inhibitors, here we studied further the structure-activity relationships (SARs) of the related class of compounds to find the lead compound.

Figure 2

2. Results and discussion

2.1 Chemistry

The synthetic route of compounds **10a-10e** was depicted in Scheme 1. 4-Chloro-4a,8a-dihydrophthalazin-1(2H)-one (**6**) was synthesized by the reported procedure[22]. Coupling of **6** with 4-fluorobenzenboronic acid by a Suzuki reaction produced intermediate **7**. Aniline ring containing intermediates **9** was generated from **7** by using sequences involving N-benzylation or Chan-Lam reaction[23] followed by nitro group reduction[24]. Then, condensation reaction of **9** with 4-(dimethylamino)butan-1-ol in the presence of triphosgene and Et_3N produced the target compounds **10a-10e**.

Scheme 1

The synthesis of compounds **11a-11d** was outlined in Scheme 2. **11a** was prepared by the condensation reaction of **9c** with the acyl chloride. Then, **11a** was reduced with $LiAlH_4$ to afford **11b**. Alternatively, the target compounds **11c** and **11d** were formed by condensation reactions of **9c** with the corresponding alcohol or amine in the presence of triphosgene and Et_3N , respectively.

Scheme 2 and 3

The synthesis of **14a-14p** was shown in Scheme 3. N-Benzoylation of phthalazinone **6** with 4-nitrobenzyl bromide followed by reduction of nitro group provided the key intermediate **12**. Intermediates **13** were obtained by carrying out Suzuki cross coupling reactions. Then, the target compounds **14a-14p** were formed by the condensation reactions of **13** with the 4-(dimethylamino)butan-1-ol in the presence of triphosgene and Et_3N .

2.2 SAR development and lead generation

The potential anti-DENV-2 activity and cytotoxicity of the synthesized phthalazinone analogues, were evaluated in Huh 7 cells. The results are summarized in Tables 1-4. The concentration of the compound that achieved 50% inhibition (IC_{50}) and 90% inhibition (IC_{90}) of DENV-2 RNA replication. The concentration of the compound killing 50% (CC_{50}) of the Huh 7 cells represented

the cytotoxicity. The selectivity index (SI), a major pharmaceutical parameter for specific antiviral activity, was determined as the ratio of CC_{50} to IC_{50} .

As shown in Table 1, *para*-substitution/*meta*-substitution (**10a**, **10b**) analogues showed good anti-DENV-2 activity with their IC_{50} values of 0.64 and 0.62 μM against DENV RNA-2 replication, respectively. However, the anti-DENV-2 activity was decreased dramatically when the carbamate group was moved from the *meta* (**10a**) to the *ortho* (**10c**) position. In addition, introducing a methyl group at the carbon atom (**10d**) or shortening the linker chain (**10e**) had negative effects on antiviral activity. It was remarkable that compound **10b**, with carbamate group on *para* position, showed the potent antiviral activity ($IC_{50} = 0.62 \mu\text{M}$) and the highest SI (30.7). Thus, compound **10b** was selected as the benchmark compound for the further optimization.

Table 1

Then, to identify the optimal side chain, modification of carbamate groups was subsequently achieved as shown in Table 2. Compound **9c**, without the carbamate group, completely lost the anti-DENV-2 activity. When the replacement of the carbamate of compound **10b** with amide, amine or carbamide produced derivatives **11a-11c**, the decreasing of anti-DENV-2 activity was observed. In addition, compound **11d** without the terminal hydrophilic dimethylamino group, decreased the maximum inhibitory activity dramatically ($IC_{90} > 80 \mu\text{M}$), indicating that the terminal hydrophilic group was important for potent antiviral activity.

Table 2

The further focused modification on the B ring of phthalazinone was achieved by introducing various heteroaryl rings. The anti-DENV-2 activity and cytotoxicity of analogues **14a-14e** were summarized in Table 3. The pyrimidyl analogue **14a**, with IC_{50} value of 0.46 μM , exhibited comparable anti-DENV-2 activities and lower cytotoxicity ($CC_{50} = 65.29 \mu\text{M}$) compared to compound **10b**. However, its maximum inhibitory activity was decreased dramatically with IC_{90} value of 62.38 μM . Replacement of phenyl with pyridyl (**14b** and **14c**) or N-methylpyrazole (**14d**), also resulted in a remarkable decreasing in antiviral potency. Furthermore, the phenyl analogue **14e** showed higher anti-DENV-2 activities and lower cytotoxicity compared to heteroaryl analogue ($IC_{50} = 2.68 \mu\text{M}$, $CC_{50} = 16.04 \mu\text{M}$).

Table 3

The further SAR exploration was mainly focused on the substituents of the phenyl moiety. As shown in Table 4. Compounds **14f-14p** all showed the comparable anti-DENV-2 activities with the variety of the substitution. Generally, compounds with the different electronic substitution at *para* and *meta* position exhibited better activity than compounds with substitution at *ortho* position. The compound **14j** or **14l** with OCH_3 or CF_3 substitution at *meta* position exhibited the significant activity than other compounds. Combined the consideration with the IC_{50} , IC_{90} and SI, Compound **14l** showed the most potency against DENV RNA replication with IC_{50} and IC_{90} values of 0.13 and 1.05 μM , respectively.

Table 4

Compound **14l** was then selected for the further evaluation of the pharmacokinetics (PK) profiles. The results of Table 5 showed that **14l** was absorbed after oral dosing at 10 mg/kg, reaching the maximum plasma concentration (C_{max}) of 94.5 ng/mL at an average time (T_{max}) of 8 h. Its oral half-time ($T_{1/2}$) and the AUC_{0-t} value were 2.91 h and 883 ng*h/mL, respectively. The average bioavailability (F) of **14l** was calculated at 34.9%.

Table 5

2.3 Molecular Docking of lead compound **14I**

Molecular docking studies were performed to investigate the binding mode between **14I** and the known anti-dengue targets including NS3 protease, capsid protein, RNA polymerase, envelop protein and methyltransferase, using Autodock vina 1.1.2 [25]. The score results showed **14I** had the strongest affinity with NS3 protease (Table S1), indicating **14I** preferred to bind with NS3 protease. As shown in Fig.3A, **14I** adopted a compact conformation to bind inside of the pocket of NS3 protease. The further analysis showed that the phthalazinone core of the **14I** was located at the hydrophobic pocket, surrounded by the residues Leu-128, Phe-130, Pro-132, Tyr-150 and Tyr-161 (Fig. 3B). A key hydrogen bond interaction was observed between the carbonyl of carbamate and the residue Gly-153 (bond distance: 2.1 Å). Moreover, the phenyl group containing trifluoromethyl formed π - π interaction with the residue Tyr-161. The above molecular simulations provided some valuable information for next target identification.

Figure 3

3. Conclusions

In conclusion, a series of novel phthalazinone derivatives based on hit **10a** were synthesized and evaluated for their *in vitro* anti-DENV RNA replication and cytotoxicity. The SAR results showed that the carbamate with a terminal hydrophilic group is crucial for its excellent antiviral activity. The SAR study and structural modification led to the discovery of the most promising compound **14I**, which displayed the potent anti-DENV activity, with IC_{50} value against DENV-2 RNA replication of 0.13 μ M and high selectivity ($SI = 89.2$). Further mechanism study and drug-like optimization of **14I** are currently under investigation. Overall, the potent activity, the synthetic ease and the desirable pharmacokinetics profiles for **14I** as an attractive lead candidate, is worthy for further investigation on the treatment of DENV infection.

4.1 General information

1H NMR and ^{13}C NMR spectral data were recorded on with Varian Mercury 500, 400 or 300 NMR spectrometer and Chemical shifts (δ) were reported in parts per million (ppm), and the signals were described as brs (broad singlet), d (doublet), dd (doublet of doublet), m (multiple), q (quarter), s (singlet), and t (triplet). Coupling constants (J values) were given in Hz. Low-resolution mass spectra (ESI) was obtained using Agilent HPLC-MS (1260-6120B) and all final compounds had purity >95% determined by using High Pressure Liquid Chromatography (HPLC) using a ZorbaxEclipse XDB-C18 column eluting with a mixture of MeCN/Water (V:V = 70: 30).

4.2 General procedure for preparation of 4-chlorophthalazin-1(2H)-one (**6**)

1,4-Dichloro-4a,8a-dihydrophthalazine (10 g, 50 mmol) was dissolved in AcOH (100 mL) and the resulting mixture was refluxed at 120 °C for 5 h. The solvent was removed under reduced pressure and the residue was washed with water (3 x 30 mL) and dried through vacuum drying oven to get crude product **6** as white solid. Yield 94% (8.50 g). 1H NMR (400 MHz, $CDCl_3$) δ 9.94 – 9.87 (m, 1H), 8.48 (d, $J = 8.0$ Hz, 1H), 8.07 (d, $J = 8.0$ Hz, 1H), 8.00 – 7.87 (m, 2H). MS (ESI) calcd for $C_8H_7ClN_2O$ $[M+H]^+$ 181.0, found 181.0

4.3 General procedure for preparation of 4-(4-fluorophenyl)phthalazin-1(2H)-one (**7**)

To a solution of **6** (8.50 g, 47.00 mmol) in 1,4-dioxane (200 mL) and H₂O (40 mL) was successively added (4-fluorophenyl)boronic acid (7.21 g, 51.50 mmol), Pd(dppf)₂Cl₂ (1.71 g, 2.34 mmol), and Cs₂CO₃ (30.00 g, 92.00 mmol). The resulting mixture was stirred at 100 °C for 12 h under argon atmosphere. Then the reaction mixture was cooled to room temperature and was concentrated in *vacuo*. Then the mixture was diluted with water and extracted with ethyl acetate. The combined organic layer was washed by saturated sodium chloride solution for three times, dried over anhydrous Na₂SO₄ and concentrated under reduced pressure. The residue was purified by silica gel chromatography to give **7** as a pale yellow solid. Yield 30% (3.60 g). ¹H NMR (400 MHz, CDCl₃) δ 8.46 (dd, *J* = 7.7, 1.1 Hz, 1H), 8.02 – 7.96 (m, 1H), 7.86 (dtd, *J* = 17.7, 7.3, 1.4 Hz, 2H), 7.36 (d, *J* = 8.4 Hz, 2H), 6.66 (d, *J* = 8.5 Hz, 2H), 5.27 (s, 2H). MS (ESI) calcd for C₁₄H₁₀FN₂O [M+H]⁺ 241.1, found 241.1

4.4 General procedure for preparation of **8**

A mixture of the corresponding bromides (1.51 mmol) and **7** (0.30 g, 1.26 mmol) in DMF (30 mL) was added with Cs₂CO₃ (0.49 g, 1.51 mmol). The reaction was stirred for 5 h at 50 °C, and then followed by dilution with water (150 mL). The mixture was extracted with ethyl acetate (50 mL × 3). The combined organic layer was washed by water for two times and saturated sodium chloride solution for one time, dried over anhydrous Na₂SO₄ and concentrated under reduced pressure. The residue was purified by silica gel chromatography to afford **8a-8d**.

4-(4-fluorophenyl)-2-(2-nitrobenzyl)phthalazin-1(2H)-one (**8a**).

Yellow oil (385mg, 81 %). ¹H NMR (400 MHz, CDCl₃) δ 8.58 – 8.53 (m, 1H), 8.38 (s, 1H), 8.17 (dd, *J* = 8.2, 1.2 Hz, 1H), 7.90 – 7.78 (m, 3H), 7.74 (dd, *J* = 6.9, 2.1 Hz, 1H), 7.64 – 7.51 (m, 3H), 7.25 (d, *J* = 8.6 Hz, 2H), 5.57 (s, 2H). MS (ESI) calcd for C₂₁H₁₅FN₃O₃ [M+H]⁺ 376.1, found 376.1

4-(4-fluorophenyl)-2-(3-nitrobenzyl)phthalazin-1(2H)-one (**8b**).

White solid (298mg, 63%). ¹H NMR (400 MHz, CDCl₃) δ 8.59 – 8.55 (m, 1H), 8.13 – 8.08 (m, 1H), 7.86 – 7.76 (m, 3H), 7.62 – 7.53 (m, 3H), 7.49 – 7.43 (m, 1H), 7.28 – 7.20 (m, 3H), 5.88 (d, *J* = 24.0 Hz, 2H). MS (ESI) calcd for C₂₁H₁₅FN₃O₃ [M+H]⁺ 376.1, found 376.1

4-(4-fluorophenyl)-2-(4-nitrobenzyl)phthalazin-1(2H)-one (**8c**).

Yellow solid (287mg, 60%). ¹H NMR (400 MHz, CDCl₃) δ 8.55 (dd, *J* = 6.8, 2.4 Hz, 1H), 8.22 (s, 1H), 7.85 – 7.81 (m, 2H), 7.75 (t, *J* = 2.8 Hz, 1H), 7.67 (d, *J* = 8.7 Hz, 2H), 7.61 – 7.55 (m, 3H), 7.24 (d, *J* = 8.6 Hz, 2H), 5.56 (s, 2H). MS (ESI) calcd for C₂₁H₁₅FN₃O₃ [M+H]⁺ 376.1, found 376.1

4-(4-fluorophenyl)-2-(1-(4-nitrophenyl)ethyl)phthalazin-1(2H)-one (**8d**)

White solid (266mg, 54%). ¹H NMR (400 MHz, CDCl₃) δ 8.57 – 8.52 (m, 1H), 8.22 – 8.16 (m, 2H), 7.78 (dddd, *J* = 9.1, 7.7, 5.8, 2.2 Hz, 3H), 7.69 (t, *J* = 8.3 Hz, 2H), 7.60 – 7.54 (m, 2H), 7.28 – 7.22 (m, 2H), 6.58 (q, *J* = 7.1 Hz, 1H), 1.91 (d, *J* = 7.1 Hz, 3H). MS (ESI) calcd for C₂₂H₁₇FN₃O₃ [M+H]⁺ 390.1, found 390.1

4.5 General procedure for preparation of 4-(4-fluorophenyl)-2-(4-nitrophenyl)phthalazin-1(2H)-one (**8e**).

To a solution of **7** (0.30 g, 2.50 mmol) in DMF (20 mL) was added (4-nitrophenyl)boronic acid (0.47 g, 5.50 mmol), pyridine (0.39 g, 10.00 mmol) and Cu(OAc)₂ (0.035 mg, 0.35 mmol). The reaction was stirred for 12 h at room temperature under oxygen atmosphere. Then the mixture was poured into water (60 mL) and was extracted with ethyl acetate (20 mL × 3). The combined organic layer was washed by water for two times and saturated sodium chloride solution for one time, dried over anhydrous Na₂SO₄ and concentrated under reduced pressure. The residue was purified by silica gel chromatography to afford **8e**. Yield 89% (400 mg). ¹H NMR (400 MHz, CDCl₃) δ 8.70 - 8.62 (m, 1H), 8.38 (t, *J* = 8.8 Hz, 4H), 8.09 (s, 1H), 7.91 - 7.88 (m, 1H), 7.82 (d, *J* = 8.8 Hz, 3H), 7.67 (dd, *J* = 8.7, 5.2 Hz, 2H). MS (ESI) calcd for C₂₀H₁₃FN₃O₃ [M+H]⁺ 362.1, found 362.1

4.6 General procedure for preparation of **10**

To a solution of **8** (1.00 mmol) in ⁱPrOH (30 mL) was added B₂Pin₂ (1.01 g, 4.00 mmol) and KO^tBu (0.028 g, 2.50 mmol). The reaction was stirred at 110 °C. After 12 h, the mixture was cooled to room temperature and was concentrated in *vacuo*. Then the mixture was diluted with water and extracted with ethyl acetate. The combined organic layer was washed by saturated sodium chloride solution for three times, dried over anhydrous Na₂SO₄ and concentrated under reduced pressure. The residue was purified by silica gel chromatography to give **9**.

To a stirred solution of **9** (0.29 mmol) and triphosgene (0.086 g, 0.33 mmol) in anhydrous dichloromethane (5 mL) at 0 °C was added triethylamine (0.12 mL, 0.87 mmol) under nitrogen atmosphere. Then a solution of 4-(dimethylamino)butan-1-ol (0.87 mmol) in dichloromethane (5 mL) was added. The mixture was stirred at room temperature overnight, diluted with dichloromethane (15 mL) and washed with water (3 × 20 mL). The organic phases were separated, combined, dried over anhydrous Na₂SO₄ and concentrated in *vacuo*. The residue was purified by using column chromatography to afford the corresponding product **10a-10e**.

4-(dimethylamino)butyl(3-((4-(4-fluorophenyl)-1-oxophthalazin-2(1H)-yl)methyl)phenyl)carbamate (**10a**).

Yellow solid (57mg, 51%, 2 steps). ¹H NMR (400 MHz, CDCl₃) δ 8.56 – 8.53 (m, 1H), 7.78 (dd, *J* = 8.8, 7.1, 3.6 Hz, 2H), 7.74 – 7.70 (m, 1H), 7.64 – 7.59 (m, 2H), 7.45 (s, 2H), 7.26 (t, *J* = 1.9 Hz, 1H), 7.24 (s, 1H), 7.22 (s, 1H), 7.20 (d, *J* = 7.7 Hz, 1H), 5.45 (s, 2H), 4.17 (t, *J* = 6.4 Hz, 2H), 2.38 – 2.31 (m, 2H), 2.27 (s, 6H), 1.70 (dd, *J* = 14.2, 6.8 Hz, 2H), 1.62 – 1.56 (m, 2H). ¹³C NMR (126 MHz, CDCl₃) δ 163.31 (d, *J* = 249.0 Hz), 159.01, 153.55, 146.19, 138.19, 137.82, 132.93, 131.49, 131.43, 131.21 (d, *J* = 3.3 Hz), 129.29, 129.15, 128.40, 127.44, 126.47, 123.57, 118.87, 118.08, 115.77, 115.60, 64.96, 59.09, 54.87, 45.24, 26.76, 23.83. MS (ESI) calcd for C₂₈H₃₀FN₄O₃ [M+H]⁺ 489.2, found 489.2

4-(dimethylamino)butyl(4-((4-(4-fluorophenyl)-1-oxophthalazin-2(1H)-yl)methyl)phenyl)carbamate (**10b**).

Yellow solid (44mg, 45%, 2 steps). ¹H NMR (400 MHz, CDCl₃) δ 8.56 – 8.52 (m, 1H), 7.77 (tt, *J* = 8.6, 3.6 Hz, 2H), 7.72 – 7.68 (m, 1H), 7.61 – 7.55 (m, 2H), 7.49 (d, *J* = 8.5 Hz, 2H), 7.37 (d, *J* = 7.7 Hz, 2H), 7.24 (t, *J* = 8.6 Hz, 2H), 5.43 (s, 2H), 4.17 (t, *J* = 6.3 Hz, 2H), 2.39 (d, *J* = 7.5 Hz, 2H), 2.29 (s, 6H), 1.69 (dd, *J* = 13.4, 6.8 Hz, 2H), 1.61 (dd, *J* = 10.2, 5.2 Hz, 2H). ¹³C NMR (126

MHz, CDCl₃) δ 163.30 (d, J = 249.0 Hz), 158.93, 153.58, 146.10, 137.56, 132.89, 131.93, 131.44 (d, J = 5.0 Hz), 131.36, 131.27, 129.67, 129.11, 128.43, 127.41, 126.42, 118.73, 115.79, 115.61, 64.88, 59.01, 54.47, 45.13, 26.70, 23.70. MS (ESI) calcd for C₂₈H₃₀FN₄O₃ [M+H]⁺ 489.2, found 489.2.

4-(dimethylamino)butyl(2-((4-(4-fluorophenyl)-1-oxophthalazin-2(1H)-yl)methyl)phenyl)carbamate (**10c**).

Yellow solid (42mg, 43 %, 2 steps). ¹H NMR (400 MHz, CDCl₃) δ 9.66 (s, 1H), 8.55 (dd, J = 7.7, 1.1 Hz, 1H), 7.89 (s, 1H), 7.83 (dd, J = 14.9, 7.2, 1.5 Hz, 2H), 7.74 (d, J = 7.8 Hz, 1H), 7.66 (dd, J = 7.7, 1.5 Hz, 1H), 7.64 – 7.59 (m, 2H), 7.38 – 7.32 (m, 1H), 7.30 (d, J = 2.1 Hz, 1H), 7.28 – 7.25 (m, 1H), 7.14 – 7.07 (m, 1H), 5.44 (s, 2H), 4.26 (t, J = 6.2 Hz, 2H), 3.09 – 3.01 (m, 2H), 2.77 (s, 6H), 1.99 (dd, J = 15.7, 8.2 Hz, 2H), 1.86 (dd, J = 13.6, 6.5 Hz, 2H). MS (ESI) calcd for C₂₈H₃₀FN₄O₃ [M+H]⁺ 489.2, found 489.2.

4-(dimethylamino)butyl(4-(1-(4-(4-fluorophenyl)-1-oxophthalazin-2(1H)-yl)ethyl)phenyl)carbamate (**10d**).

Yellow solid (59mg, 48%, 2 steps). ¹H NMR (400 MHz, CDCl₃) δ 8.53 (dd, J = 6.3, 2.7 Hz, 1H), 7.79 – 7.71 (m, 3H), 7.59 – 7.54 (m, 2H), 7.48 (d, J = 8.6 Hz, 2H), 7.40 (d, J = 8.4 Hz, 2H), 7.23 (t, J = 8.7 Hz, 2H), 6.48 (q, J = 7.1 Hz, 1H), 4.16 (t, J = 6.1 Hz, 2H), 2.84 – 2.78 (m, 2H), 2.61 (s, 6H), 1.84 (s, 2H), 1.83 (d, J = 7.1 Hz, 3H), 1.76 – 1.68 (m, 2H). MS (ESI) calcd for C₂₉H₃₂FN₄O₃ [M+H]⁺ 503.2, found 503.2.

4-(Dimethylamino)butyl(4-(4-(4-fluorophenyl)-1-oxo-1,8a-dihydrophthalazin-2(4aH)-yl)phenyl)carbamate (**10e**)

Yellow solid (55mg, 53%, 2 steps) ¹H NMR (400 MHz, CDCl₃) δ 8.66 – 8.60 (m, 1H), 7.84 (dq, J = 7.1, 5.5 Hz, 2H), 7.77 (d, J = 7.1 Hz, 1H), 7.70 – 7.63 (m, 4H), 7.53 (d, J = 8.3 Hz, 2H), 7.24 (t, J = 8.7 Hz, 2H), 4.22 (t, J = 6.4 Hz, 2H), 2.43 (d, J = 7.5 Hz, 2H), 2.33 (s, 6H), 1.77 – 1.71 (m, 2H), 1.66 (d, J = 7.1 Hz, 2H). MS (ESI) calcd for C₂₇H₂₈FN₄O₃ [M+H]⁺ 475.2, found 475.2

4.7 General procedure for preparation of 4-(dimethylamino)-N-(4-((4-(4-fluorophenyl)-1-oxophthalazin-2(1H)-yl)methyl)phenyl)butanamide (11a)

To a stirred solution of 4-(dimethylamino)butanoic acid (70 mg, 0.42 mmol) in anhydrous dichloromethane (10 mL) at 0 °C was added oxalyl chloride (0.11 mL, 1.25 mmol) and DMF (*cat*). After 3 h, the solvent was removed under reduced pressure and the residue was dissolved with anhydrous THF (10 mL) to get acyl chloride intermediate. Then acyl chloride intermediate was slowly added to the solution of **9c** (97mg, 0.35mmol) and Et₃N (0.12 mL, 0.83 mmol) at 0 °C. The organic phases were separated, combined, dried over anhydrous Na₂SO₄ and concentrated in vacuo. The residue was purified by using column chromatography to afford the **11a**.

Yellow solid (98mg, 61%). ¹H NMR (400 MHz, CDCl₃) δ 9.86 (s, 1H), 8.51 (dd, J = 6.8, 2.5 Hz, 1H), 7.76 (ddt, J = 9.8, 7.1, 3.4 Hz, 2H), 7.69 (dt, J = 6.5, 3.2 Hz, 1H), 7.56 (ddd, J = 17.4, 8.7, 5.3 Hz, 4H), 7.47 (d, J = 8.5 Hz, 2H), 7.26-7.19 (m, 2H), 5.42 (s, 2H), 2.51 (dd, J = 14.2, 7.3 Hz,

4H), 2.37 (s, 6H), 1.94 - 1.86 (m, 2H). ^{13}C NMR (126 MHz, CDCl_3) δ 171.21, 163.30 (d, J = 248.9 Hz), 158.93, 146.11, 138.35, 132.91, 132.20, 131.45 (d, J = 5.4 Hz), 131.36, 131.23 (d, J = 3.2 Hz), 129.44, 129.10, 128.40, 127.36, 126.43, 119.57, 115.79, 115.61, 58.59, 54.59, 44.66, 36.07, 22.35. MS (ESI) calcd for $\text{C}_{27}\text{H}_{28}\text{FN}_4\text{O}_2$ $[\text{M}+\text{H}]^+$ 459.2, found 459.2.

4.8 General procedure for preparation of 2-(4-((4-(dimethylamino)butyl)amino)benzyl)-4-(4-fluorophenyl)phthalazin-1(2H)-one (**11b**)

To a solution of **11a** (90 mg, 0.20 mmol) in anhydrous THF (20 mL) was added LiAlH_4 (9 mg, 0.24 mmol) at refluxing. After 2 hours, the solvent was removed under reduced pressure. The residue was purified by using column chromatography to afford the **11b**.

Yellow solid (70mg, 78%). ^1H NMR (400 MHz, CDCl_3) δ 8.54 (d, J = 7.4 Hz, 1H), 7.81 - 7.68 (m, 3H), 7.62 - 7.53 (m, 3H), 7.40 (d, J = 8.5 Hz, 2H), 7.23 (dd, J = 18.4, 9.8 Hz, 2H), 6.61 (s, 1H), 5.36 (s, 2H), 3.21 (dd, J = 13.3, 6.6 Hz, 2H), 3.03 - 2.95 (m, 2H), 2.77 (s, 6H), 1.97 (d, 2H), 1.74 (d, J = 6.9 Hz, 2H). MS (ESI) calcd for $\text{C}_{27}\text{H}_{30}\text{FN}_4\text{O}$ $[\text{M}+\text{H}]^+$ 445.2, found 445.2.

4.9 General procedure for preparation of **11c-11d**

To a stirred solution of **9c** (43 mg, 0.20 mmol) and triphosgene (36 mg, 0.20 mmol) in anhydrous dichloromethane (5 mL) at 0 °C was added triethylamine (60 mg, 0.60 mmol) under nitrogen atmosphere. Then a solution of N,N-dimethylbutane-1,4-diamine (0.085 mL, 0.60 mmol) or n-butanol (0.052 mL, 0.60 mmol) in dichloromethane (5 mL) was added. The mixture was stirred at room temperature for overnight, and then diluted with dichloromethane (15 mL). The organic phases was washed with water (3 × 20 mL) and dried over anhydrous Na_2SO_4 and concentrated in *vacuo*. The residue was purified by using column chromatography to afford the corresponding product **11c-11d**.

1-(4-(dimethylamino)butyl)-3-(4-((4-(4-fluorophenyl)-1-oxophthalazin-2(1H)-yl)methyl)phenyl)urea (**11c**)

Yellow solid (55mg, 56%). ^1H NMR (400 MHz, CDCl_3) δ 8.51 (d, J = 7.8 Hz, 1H), 7.84 - 7.69 (m, 3H), 7.64 - 7.53 (m, 2H), 7.44 - 7.33 (m, 3H), 7.27 - 7.20 (m, 3H), 5.40 (s, 2H), 3.21 (s, 2H), 2.56 (s, 2H), 2.30 (s, 2H), 2.21 (s, 6H), 1.51 (s, 4H). MS (ESI) calcd for $\text{C}_{28}\text{H}_{31}\text{FN}_5\text{O}_2$ $[\text{M}+\text{H}]^+$ 488.2, found 488.2.

butyl 4-((4-(4-fluorophenyl)-1-oxophthalazin-2(1H)-yl)methyl)phenyl)carbamate (**11d**)

Yellow solid (60mg, 61%). ^1H NMR (400 MHz, CDCl_3) δ 8.55 (dd, J = 7.2, 2.1 Hz, 1H), 7.82 - 7.74 (m, 2H), 7.72 - 7.68 (m, 1H), 7.61 - 7.55 (m, 2H), 7.50 (d, J = 8.5 Hz, 2H), 7.36 (d, J = 8.3 Hz, 2H), 7.27 - 7.21 (m, 2H), 5.43 (s, 2H), 4.17 (t, J = 6.7 Hz, 2H), 1.65 (d, J = 7.8 Hz, 2H), 1.42 (dd, J = 15.1, 7.5 Hz, 2H), 0.96 (t, J = 7.4 Hz, 3H). ^{13}C NMR (126 MHz, CDCl_3) δ 165.20 (d, J = 249.1 Hz), 160.84, 155.58, 148.01, 139.54, 134.80, 133.74, 133.35 (d, J = 5.2 Hz), 133.26, 133.15 (d, J = 3.2 Hz), 131.59, 131.00, 130.33, 129.32, 128.33, 120.53, 117.70, 117.52, 67.02, 56.39, 32.85, 20.97, 15.63. MS (ESI) calcd for $\text{C}_{26}\text{H}_{25}\text{FN}_3\text{O}_3$ $[\text{M}+\text{H}]^+$ 446.2, found 446.2.

4.10 General procedure for preparation of 2-(4-Aminobenzyl)-4-chlorophthalazin-1(2H)-one (**12**)

To a solution of **6** (3.00 g, 12.50 mmol) was added 1-bromo-4-(nitromethyl)benzene (3.24 g, 15.00 mmol) and Cs_2CO_3 (4.89 g, 15.00 mmol). The reaction mixture was stirred at 50 °C. After 5 h, the mixture was poured into water (100 mL) and then was extracted with ethyl acetate (100 mL

×3). The combined organic layer was washed by water for two times and saturated sodium chloride solution for one time, dried over anhydrous Na₂SO₄ and concentrated under reduced pressure. The crude product was further reacted directly for next step without purification. The crude product above (3.00 g, 9.50 mmol) was dissolved in ¹PrOH (100 mL), the solution was added with B₂Pin₂(14.47 g, 57.00 mmol), KO^tBu (2.56 g, 22.80 mmol). The reaction was stirred at 110 °C. After 12 h, the reaction mixture was cooled to room temperature and was concentrated in *vacuo*. Then the mixture was diluted with water and extracted with ethyl acetate. The combined organic layer was washed by saturated sodium chloride solution for three times, dried over anhydrous Na₂SO₄ and concentrated under reduced pressure. The residue was purified by silica gel chromatography to give **12**.

Yellow solid (2.15g, 60%, 2 steps). ¹H NMR (400 MHz, CDCl₃) δ 8.59 – 8.55 (m, 1H), 8.13 – 8.08 (m, 1H), 7.86 – 7.76 (m, 3H), 7.62 – 7.53 (m, 3H), 7.49 – 7.43 (m, 1H), 7.28 – 7.20 (m, 3H), 5.88 (d, *J* = 24.0 Hz, 2H). MS (ESI) calcd for C₁₅H₁₃ClN₃O [M+H]⁺ 286.1, found 286.1.

4.11 General procedure for preparation of **14a-14r**

12 (100 mg, 0.35 mmol) was dissolved in the mixture of 1,4-dioxane (10 mL) and H₂O (2.00 mL) and then added with boronic acid (2.80 mmol), Pd(dppf)₂Cl₂ (28 mg, 0.035 mmol) and Cs₂CO₃ (228 mg, 0.70 mmol). The reaction was heated at 100 °C under argon atmosphere. After 12h, the reaction mixture was cooled to room temperature and was concentrated in *vacuo*. Then the mixture was diluted with water and extracted with ethyl acetate. The combined organic layer was washed by saturated sodium chloride solution for three times, dried over anhydrous Na₂SO₄ and concentrated under reduced pressure. The residue was purified by silica gel chromatography to give **13**.

To a stirred solution of **13** and triphosgene (100 mg, 0.34 mmol) in anhydrous dichloromethane (5 mL) was added triethylamine (104 mg, 1.02 mmol) at 0 °C under nitrogen atmosphere. After 5 minutes, a solution of 4-(dimethylamino)butan-1-ol (1.02 mmol) in dichloromethane (5.00 mL) was added and then the mixture was stirred at room temperature for overnight. The reaction was diluted with dichloromethane (15 mL) and washed with water (3×20 mL). The organic phases were dried over anhydrous Na₂SO₄ and concentrated in *vacuo*. The residue was purified by using column chromatography to afford the corresponding product.

4-(Dimethylamino)butyl 4-((1-oxo-4-(pyrimidin-5-yl)phthalazin-2(1H)-yl)methyl)phenyl)carbamate (**14a**)

Yellow solid (62mg, 42%, 2 steps). ¹H NMR (400 MHz, CDCl₃) δ 9.38 (s, 1H), 9.02 (s, 2H), 8.58 (dd, *J* = 6.3, 2.8 Hz, 1H), 7.87 – 7.83 (m, 2H), 7.67 (dd, *J* = 6.6, 2.6 Hz, 1H), 7.49 (d, *J* = 8.5 Hz, 2H), 7.41 (d, *J* = 8.5 Hz, 2H), 5.44 (d, *J* = 5.7 Hz, 2H), 4.20 (t, *J* = 6.2 Hz, 2H), 2.85 – 2.78 (m, 2H), 2.63 (s, 6H), 1.87 (d, *J* = 7.3 Hz, 2H), 1.77 (dd, *J* = 13.6, 6.6 Hz, 2H). MS (ESI) calcd for C₂₆H₂₉N₆O₃ [M+H]⁺ 473.2, found 473.2

4-(Dimethylamino)butyl 4-((1-oxo-4-(pyridin-4-yl)phthalazin-2(1H)-yl)methyl)phenyl)carbamate (**14b**)

Yellow solid (59mg, 36%, 2 steps). ¹H NMR (400 MHz, CDCl₃) δ 8.81 (dd, *J* = 4.5, 1.5 Hz, 2H), 8.58 – 8.53 (m, 1H), 7.85 – 7.77 (m, 2H), 7.74 – 7.70 (m, 1H), 7.55 (dd, *J* = 4.4, 1.6 Hz, 2H), 7.49 (d, *J* = 8.5 Hz, 2H), 7.36 (d, *J* = 8.0 Hz, 2H), 5.43 (s, 2H), 4.16 (dd, *J* = 6.5, 4.2 Hz, 2H), 2.32 – 2.29 (m, 2H), 2.22 (s, 6H), 1.68 (d, *J* = 5.8 Hz, 2H), 1.57 (d, *J* = 7.2 Hz, 2H). ¹³C NMR (126 MHz, CDCl₃) δ 160.76, 155.43, 152.13,

146.28, 144.77, 139.55, 135.08, 133.70, 133.46, 131.66, 130.30, 130.19, 129.55, 127.65, 125.99, 120.53, 67.02, 61.15, 56.48, 47.37, 28.73, 25.97. MS (ESI) calcd for $C_{27}H_{30}N_5O_3$ $[M+H]^+$ 472.2, found 472.2.

4-(Dimethylamino)butyl 4-((1-oxo-4-(pyridin-3-yl)phthalazin-2(1H)-yl)methyl)phenyl)carbamate (**14c**)

Yellow solid (66mg, 40%, 2 steps). 1H NMR (400 MHz, $CDCl_3$) δ 9.38 (s, 1H), 9.02 (s, 2H), 8.58 (dd, $J = 6.3, 2.8$ Hz, 1H), 7.87 – 7.83 (m, 2H), 7.67 (dd, $J = 6.6, 2.6$ Hz, 1H), 7.49 (d, $J = 8.5$ Hz, 2H), 7.41 (d, $J = 8.5$ Hz, 2H), 5.44 (d, $J = 5.7$ Hz, 2H), 4.20 (t, $J = 6.2$ Hz, 2H), 2.85 – 2.78 (m, 2H), 2.63 (s, 6H), 1.87 (d, $J = 7.3$ Hz, 2H), 1.77 (dd, $J = 13.6, 6.6$ Hz, 2H). MS (ESI) calcd for $C_{27}H_{30}N_5O_3$ $[M+H]^+$ 472.2, found 472.2.

4-(Dimethylamino)butyl 4-((4-(1-methyl-1H-pyrazol-4-yl)-1-oxophthalazin-2(1H)-yl)methyl)phenyl)carbamate (**14d**)

Yellow solid (70mg, 42%, 2 steps) 1H NMR (400 MHz, $CDCl_3$) δ 8.53 (dd, $J = 6.0, 3.3$ Hz, 1H), 7.98 (dd, $J = 6.3, 3.0$ Hz, 1H), 7.85 (s, 1H), 7.83 – 7.78 (m, 2H), 7.76 (s, 1H), 7.48 (d, $J = 8.5$ Hz, 2H), 7.38 (d, $J = 7.7$ Hz, 2H), 5.40 (s, 2H), 4.18 (t, $J = 5.9$ Hz, 2H), 4.04 (s, 3H), 2.69 (d, $J = 8.1$ Hz, 2H), 2.54 (s, 6H), 1.74 (d, $J = 6.1$ Hz, 4H). MS (ESI) calcd for $C_{26}H_{31}N_6O_3$ $[M+H]^+$ 475.2, found 475.2.

4-(Dimethylamino)butyl(4-((1-oxo-4-phenylphthalazin-2(1H)-yl)methyl)phenyl)carbamate(**14e**) Yellow solid (66mg, 40%, 2 steps) 1H NMR (400 MHz, $CDCl_3$) δ 8.54 (d, $J = 7.2$ Hz, 1H), 7.76 (dt, $J = 12.7, 3.9$ Hz, 3H), 7.62 – 7.47 (m, 7H), 7.37 (d, $J = 8.0$ Hz, 2H), 5.44 (s, 2H), 4.17 (t, $J = 6.3$ Hz, 2H), 2.44 – 2.38 (m, 2H), 2.31 (s, 6H), 1.65 (ddd, $J = 26.7, 11.1, 5.6$ Hz, 4H). MS (ESI) calcd for $C_{28}H_{31}N_4O_3$ $[M+H]^+$ 471.2, found 471.2.

4-(Dimethylamino)butyl 4-((4-(4-methoxyphenyl)-1-oxophthalazin-2(1H)-yl)methyl)phenyl)carbamate (**14f**)

Yellow solid (90mg, 52%, 2 steps). 1H NMR (400 MHz, $CDCl_3$) δ 8.56 – 8.49 (m, 1H), 7.78 – 7.73 (m, 3H), 7.55 – 7.46 (m, 4H), 7.35 (d, $J = 8.0$ Hz, 2H), 7.08 – 7.04 (m, 2H), 5.41 (d, $J = 8.6$ Hz, 2H), 4.16 (t, $J = 6.5$ Hz, 2H), 3.90 (s, 3H), 3.56 (d, $J = 5.5$ Hz, 2H), 2.26 (s, 6H), 1.67 (dd, $J = 4.7, 2.4$ Hz, 4H). MS (ESI) calcd for $C_{29}H_{33}N_4O_4$ $[M+H]^+$ 501.2, found 501.2.

4-(Dimethylamino)butyl(4-((4-(4-cyanophenyl)-1-oxophthalazin-2(1H)-yl)methyl)phenyl)carbamate (**14g**)

Yellow solid (80mg, 46%, 2 steps). 1H NMR (400 MHz, $CDCl_3$) δ 8.58 – 8.54 (m, 1H), 7.86 – 7.76 (m, 4H), 7.75 – 7.72 (m, 2H), 7.66 (dd, $J = 7.4, 1.7$ Hz, 1H), 7.48 (d, $J = 8.5$ Hz, 2H), 7.37 (d, $J = 8.2$ Hz, 2H), 5.42 (s, 2H), 4.17 (t, $J = 6.3$ Hz, 2H), 2.44 – 2.38 (m, 2H), 2.32 (s, 6H), 1.73 – 1.68 (m, 2H), 1.63 (dd, $J = 10.3, 5.4$ Hz, 2H). MS (ESI) calcd for $C_{29}H_{30}N_5O_3$ $[M+H]^+$ 496.2, found 496.2.

4-(Dimethylamino)butyl 4-((1-oxo-4-(4-(trifluoromethyl)phenyl)phthalazin-2(1H)-yl)methyl)phenyl)carbamate (**14h**)

Yellow solid (66mg, 35%, 2 steps). 1H NMR (400 MHz, $CDCl_3$) δ 8.57 – 8.54 (m, 1H), 7.82 (s, 1H), 7.80 (d, $J = 2.6$ Hz, 2H), 7.78 (dd, $J = 8.0, 1.7$ Hz, 1H), 7.74 (d, $J = 2.6$ Hz, 1H), 7.72 (s, 1H), 7.68 (dd, $J = 7.4, 1.8$ Hz, 1H), 7.49 (d, $J = 8.5$ Hz, 2H), 7.38 (dd, $J = 12.6, 7.2$ Hz, 2H), 5.43 (s, 2H), 4.17 (t, $J = 6.6$ Hz, 2H), 2.28 (d, $J = 9.0$ Hz, 2H), 2.22 (s, 6H), 1.68 (dd, $J = 14.8, 6.8$ Hz, 2H), 1.56 (td, $J = 8.2, 4.3$ Hz, 2H). MS (ESI) calcd for $C_{29}H_{30}F_3N_4O_3$ $[M+H]^+$ 539.2, found 539.2.

4-(Dimethylamino)butyl 4-((4-(3-fluorophenyl)-1-oxophthalazin-2(1H)-yl)methyl)phenyl)carbamate (**14i**)

Yellow solid (65mg, 38%, 2 steps). ^1H NMR (400 MHz, CDCl_3) δ 8.54 (dd, $J = 6.7$, 2.1 Hz, 1H), 7.80 – 7.71 (m, 3H), 7.50 (dd, $J = 11.4$, 5.0 Hz, 3H), 7.34 (ddd, $J = 10.9$, 10.2, 4.7Hz, 5H), 7.23 (td, $J = 8.4$, 1.7 Hz, 1H), 5.43 (s, 2H), 4.17 (t, $J = 6.5$ Hz, 2H), 2.31 – 2.26 (m, 2H), 2.22 (s, 6H), 1.72 – 1.67 (m, 2H), 1.59 – 1.52 (m, 2H). MS (ESI) calcd for $\text{C}_{28}\text{H}_{30}\text{FN}_4\text{O}_3$ $[\text{M}+\text{H}]^+$ 489.2, found 489.2.

4-(Dimethylamino)butyl 4-((4-(3-methoxyphenyl)-1-oxophthalazin-2(1H)-yl)methyl)phenyl)carbamate (**14j**)

Yellow solid (72mg, 41%, 2 steps). ^1H NMR (400 MHz, CDCl_3) δ 8.52 (d, $J = 7.8$ Hz, 1H), 7.76 (t, $J = 6.8$ Hz, 3H), 7.47 (t, $J = 8.1$ Hz, 3H), 7.44 – 7.40 (m, 2H), 7.16 (d, $J = 7.5$ Hz, 1H), 7.11 (s, 1H), 7.06 (d, $J = 8.1$ Hz, 1H), 5.42 (s, 2H), 4.16 (t, $J = 6.0$ Hz, 2H), 3.88 (s, 3H), 2.82 – 2.74 (m, 2H), 2.59 (s, 6H), 1.83 (d, $J = 7.7$ Hz, 2H), 1.74 – 1.69 (m, 2H). MS (ESI) calcd for $\text{C}_{29}\text{H}_{33}\text{N}_4\text{O}_4$ $[\text{M}+\text{H}]^+$ 501.2, found 501.2.

4-(Dimethylamino)butyl 4-((4-(3-cyanophenyl)-1-oxophthalazin-2(1H)-yl)methyl)phenyl)carbamate (**14k**)

Yellow solid (85mg, 49%, 2 steps). ^1H NMR (400 MHz, CDCl_3) δ 8.58 – 8.54 (m, 1H), 7.91 (t, $J = 1.4$ Hz, 1H), 7.87 – 7.79 (m, 4H), 7.71 – 7.67 (m, 1H), 7.66 – 7.62 (m, 1H), 7.48 (d, $J = 8.6$ Hz, 2H), 7.36 (d, $J = 8.3$ Hz, 2H), 5.43 (s, 2H), 4.17 (t, $J = 6.6$ Hz, 2H), 2.32 – 2.27 (m, 2H), 2.23 (d, $J = 2.8$ Hz, 6H), 1.74 – 1.65 (m, 2H), 1.60 – 1.51 (m, 2H). MS (ESI) calcd for $\text{C}_{29}\text{H}_{30}\text{N}_5\text{O}_3$ $[\text{M}+\text{H}]^+$ 496.2, found 496.2.

4-(Dimethylamino)butyl 4-((1-oxo-4-(3-(trifluoromethyl)phenyl)phthalazin-2(1H)-yl)methyl)phenyl)carbamate (**14l**)

Yellow solid (85mg, 45%, 2 steps). ^1H NMR (400 MHz, CDCl_3) δ 8.58 – 8.53 (m, 1H), 7.87 (s, 1H), 7.82 – 7.75 (m, 4H), 7.71 – 7.63 (m, 2H), 7.49 (d, $J = 8.5$ Hz, 2H), 7.37 (d, $J = 8.2$ Hz, 2H), 5.43 (s, 2H), 4.17 (t, $J = 6.4$ Hz, 2H), 2.41 – 2.35 (m, 2H), 2.29 (s, 6H), 1.70 (dt, $J = 12.8$, 6.5 Hz, 2H), 1.65 – 1.57 (m, 2H). ^{13}C NMR (126 MHz, CDCl_3) δ 158.89, 153.56, 145.51, 137.63, 136.01, 133.11, 132.89, 131.77, 131.66, 131.28, 131.02, 129.71, 129.21, 128.79, 128.44, 127.56, 126.38 (d, $J = 3.7$ Hz), 126.05, 125.89 (d, $J = 3.6$ Hz), 123.90 (q, $J = 272.5$ Hz), 118.75, 64.87, 58.99, 54.58, 45.10, 26.68, 23.66. MS (ESI) calcd for $\text{C}_{29}\text{H}_{30}\text{F}_3\text{N}_4\text{O}_3$ $[\text{M}+\text{H}]^+$ 539.2, found 539.2. HRMS (ESI) calcd for $\text{C}_{29}\text{H}_{30}\text{F}_3\text{N}_4\text{O}_3$ $[\text{M}+\text{H}]^+$ 539.2265, found 539.2270.

4-(Dimethylamino)butyl 4-((4-(2-fluorophenyl)-1-oxophthalazin-2(1H)-yl)methyl)phenyl)carbamate (**14m**)

Yellow solid (68mg, 40%, 2 steps). ^1H NMR (400 MHz, CDCl_3) δ 8.58 – 8.53 (m, 1H), 7.87 (s, 1H), 7.82 – 7.75 (m, 4H), 7.71 – 7.63 (m, 2H), 7.49 (d, $J = 8.5$ Hz, 2H), 7.37 (d, $J = 8.2$ Hz, 2H), 5.43 (s, 2H), 4.17 (t, $J = 6.4$ Hz, 2H), 2.41 – 2.35 (m, 2H), 2.29 (s, 6H), 1.70 (dt, $J = 12.8$, 6.5 Hz, 2H), 1.65 – 1.57 (m, 2H). ^{13}C NMR (126 MHz, CDCl_3) δ 162.19 (d, $J = 249.3$ Hz), 160.99, 144.58, 139.42, 134.85, 133.75, 133.43, 133.23 (d, $J = 8.0$ Hz), 131.52, 131.35, 129.91, 128.96, 128.30, 126.54 (d, $J = 3.4$ Hz), 124.98, 124.86, 120.58, 118.04, 117.87, 66.87, 61.01, 56.50, 47.17, 28.65, 25.74. MS (ESI) calcd for $\text{C}_{28}\text{H}_{30}\text{FN}_4\text{O}_3$ $[\text{M}+\text{H}]^+$ 489.2, found 489.2.

4-(Dimethylamino)butyl 4-((4-(2-methoxyphenyl)-1-oxophthalazin-2(1H)-yl)methyl)phenyl)carbamate (**14n**)

Yellow solid (96mg, 55%, 2 steps). ^1H NMR (400 MHz, CDCl_3) δ 8.48 (d, $J = 7.8$ Hz, 1H), 7.70 (dt, $J = 13.7$, 6.5 Hz, 2H), 7.54 – 7.45 (m, 3H), 7.39 – 7.31 (m, 4H), 7.13 (t, $J = 7.4$ Hz, 1H), 7.06 (d, $J = 8.3$ Hz, 1H), 5.55 (d, $J = 13.8$ Hz, 1H), 5.30 (d, $J = 13.2$ Hz, 1H), 4.17 (t, $J = 6.4$ Hz,

2H), 3.74 (s, 3H), 2.33 (d, $J = 7.4$ Hz, 2H), 2.26 (s, 6H), 1.69 (d, $J = 7.2$ Hz, 2H), 1.59 (d, $J = 7.1$ Hz, 2H). MS (ESI) calcd for $C_{29}H_{33}N_4O_4$ $[M+H]^+$ 501.2, found 501.2.

4-(Dimethylamino)butyl 4-((4-(2-cyanophenyl)-1-oxophthalazin-2(1H)-yl)methyl)phenyl)carbamate (**14o**)

Yellow solid (89mg, 51%, 2 steps). 1H NMR (400 MHz, $CDCl_3$) δ 8.55 (d, $J = 7.5$ Hz, 1H), 7.91 (d, $J = 7.9$ Hz, 1H), 7.79 (dd, $J = 14.3, 7.9$ Hz, 3H), 7.65 (dd, $J = 16.8, 7.4$ Hz, 2H), 7.52 (d, $J = 8.6$ Hz, 2H), 7.45 (d, $J = 8.2$ Hz, 1H), 7.39 (s, 2H), 5.45 (s, 2H), 4.19 (s, 2H), 2.78 (s, 2H), 2.60 (s, 6H), 1.85 (s, 2H), 1.75 (s, 2H). MS (ESI) calcd for $C_{29}H_{30}N_5O_3$ $[M+H]^+$ 496.2, found 496.2.

4-(Dimethylamino)butyl 4-((1-oxo-4-(2-(trifluoromethyl)phenyl)phthalazin-2(1H)-yl)methyl)phenyl)carbamate (**14p**)

Yellow solid (81mg, 46%, 2 steps). 1H NMR (400 MHz, $CDCl_3$) δ 8.47 (d, $J = 5.9$ Hz, 1H), 8.20 (s, 1H), 7.74 (dd, $J = 14.5, 10.8$ Hz, 3H), 7.59 (dd, $J = 15.5, 10.5$ Hz, 3H), 7.38 (d, $J = 7.3$ Hz, 1H), 7.20 (dt, $J = 16.4, 8.2$ Hz, 3H), 7.02 (d, $J = 7.3$ Hz, 1H), 5.40 (s, 2H), 3.16 (s, 2H), 2.75 (d, $J = 13.2$ Hz, 2H), 2.59 (s, 6H), 1.70 (s, 2H), 1.49 (d, $J = 6.2$ Hz, 2H). MS (ESI) calcd for $C_{29}H_{30}F_3N_4O_3$ $[M+H]^+$ 539.2, found 539.2.

4.12 Anti-DV2 activity test of SAR research

The antiviral activity of compound was tested using an clinical infectious DENV-2 virus strain (D2Y98P strain, serotype II).

Virus was propagated in C6/36 cells. C6/36 cells were cultured in RPMI-1640 medium with 5% FBS, 28 °C, 5% CO₂. Cells were re-seeded into T75 flask before inoculated with virus for 2 hours. Medium was refreshed (5% FBS RPMI 1640) and infected cells were cultured under 33 °C for 6 days. Virus stock solution was purified and concentrated. Virus was tittered in BHK cells by plaque formation assay.

For compound anti-DV2 test in Huh7 cells, which is a human hepatocarcinoma cell line. Huh7 cells were cultured in high glucose DMEM medium with 10% FBS, 37 °C, 5% CO₂. Before compound anti-DV2 test, 4×10^4 Huh7 cells were seeded into 96 well plate with 2% FBS DMEM and cultured overnight. Cells were then infected with DENV-2 virus at MOI=2 for 2 hrs. Multiplicity of infection (MOI) is the ratio of infectious virus particles versus cell number, therefore, MOI=2 means nearly all cells were infected by virus initially, this produces one round of virus replication cycle in the cell culture, no second round infection by progeny virus. Virus inoculation was washed out and replaced with fresh medium after initial infection and compounds were added at demand concentration. After 48 hrs, cell culture supernatant were collected for viral genomic RNA quantification by method described below. Cytotoxic effect of compounds were assayed by MTT method which evaluated the reduction product of MTT by cellular succinate dehydrogenase as an indicator of cell liability. CC50 indicates the concentration of compound at which reducing the readout to half of the no compound control.

Supernatant DV2 viral genomic RNA was quantified by one-step qRT-PCR method. DV2 viral genomic RNA in cell culture supernatant were first extracted by Qiasymphony SP/AS automatic nucleic acid purification station (QIASymphony Virus/Bacteria Mini Kit, Cellfree200 default IC protocol, 110 μ L eluent). One-step quantification PCR was set up using Quantitect Multiplex RT-PCR kit according to manual. Pure viral RNA containing viral 3'UTR region obtained by in vitro transcription from cloned plasmid was used as standard to evaluate absolute viral genomic RNA quantity in cell culture supernatant. IC90 and IC50 are compound concentrations needed to

reduce viral RNA quantities by 90% and 50% respectively. Primers and Taqman probes were synthesized by Thermo using sequence listed below:

qDV2Lab3UTR/Sp: TGTAGCTCCACCTGAGAAGG

qDV2Lab3UTR/Asp: CATTGTTGCTGCGATTTGTA

qDV2Lab3UTR/Probe: FAM-CCATGGTTTGTGGCCTCCCA-BQ1

4.13 Experimental protocol for the pharmacokinetic study

Six naive male CD-1 mice weighing 18 to 22 g were divided randomly into 2 groups, Mice were housed under standard conditions and had ad libitum access to water and a standard laboratory diet.

Each mouse was housed individually in a mouse metabolic cage and was not restrained at any time during the study. The mice were starved for 12 h before the experiments with the exception of free access to water and were fed 2h after administration.

The oroling solution was prepared by dissolving appropriate amount in 0.5% MC (without DMSO). For IV route, **141** was dissolved in 5% DMSO, then added respectively EtOH, PEG300 and saline (5/40/50, v/v/v) in the solution. The drug solution was sampled (before and after administration, 50 μ L mixed with 50 μ L DMSO) to be measured.

Blood samples (25 μ L each) were collected from the femoral vein at scheduled time point (0.25, 0.5, 1, 2, 4, 8, 24 h for PO and at 3 min, 0.25, 0.75, 2, 4, 8, 24 h for IV) with EDTA as anticoagulant. The blood was centrifuged immediately at 11000 rpm for 5 mins. 10 μ L plasma was transferred into a new centrifuge tube with a pre added PK-IS solution of 100 μ L (methanol: acetonitrile (1:1, v/v)) immediately, which was mixed well and stored at -20°C to be measured.

Pharmacokinetic parameters including half-life ($t_{1/2}$), maximum plasma time (t_{max}), concentration (C_{max}), area under concentration–time curve (AUC_{last} and AUC_{inf}), clearance (CL), steady-state volume of distribution (V_{ss}), bioavailability(F), pharmacokinetic parameters were analyzed by non-compartmental method using WinNonlin Version 6.4 (Pharsight Corporation, Mountain View, USA).

ACKNOWLEDGMENT. This work was supported by grants from National Key Research and Development Program of China (2016YFC1200400), and Defense Technology Innovation Fund, Chinese Academy of Sciences (CXJJ-17-Q147), and National Natural Science Foundation of China(81502914).

References

- [1] JG. Rigau-Pérez, GG. Clark, DJ. Gubler, P. Reiter, EJ. Sanders, AV. Vorndam, Dengue and dengue haemorrhagic fever. *Lancet*. 352 (1999) 971-977.
- [2] DJ. Gubler, The economic burden of dengue. *Am. J. Trop. Med. Hyg.* 86 (2012) 743-744.
- [3] G. Screaton, J. Mongkolsapaya, S. Yacoub, C. Roberts. New insights into the immunopathology and control of dengue virus infection. *Nat Rev Immunol.* 15 (2015) 745-59.
- [4] KI. Hidari, T. Suzuki, Dengue virus receptor. *Trop MedHealth.* 39 (2011) 37-43.
- [5] YY. Cheung, KC. Chen, H. Chen, EK. Seng, JJ. Chu. Antiviral activity of lanatoside C against dengue virus infection. *Antiviral Res.* 111 (2014) 93-99.

- [6] J. Whitehorn, CP. Simmons, The pathogenesis of dengue. *Vaccine*. 29 (2011) 7221-7228.
- [7] MG. Guzman, M. Alvarez, SB. Halstead, Secondary infection as a risk factor for dengue hemorrhagic fever/dengue shock syndrome: an historical perspective and role of antibody-dependent enhancement of infection. *Arch. Virol.* 158 (2013) 1445-1459.
- [8] The data was cited in the WHO website: <http://www.who.int/mediacentre/factsheets/fs117/en/>
- [9] S. Bhakat, W. Karubiu, V. Jayaprakash, ME. Soliman. A perspective on targeting non-structural proteins to combat neglected tropical diseases: Dengue, West Nile and Chikungunya viruses. *Eur. J. Med. Chem.* 87 (2014) 677-702.
- [10] H. Beesetti, N. Khanna, S. Swaminathan, Drugs for dengue: a patent review (2010 – 2014). *Expert. Opin. Ther. Pat.* 24 (2014) 1171-1184.
- [11] S. Kaptein and J. Neyts, Towards antiviral therapies for treating dengue virus infections. *Curr. Opin. Pharmacol.* 30 (2016) 1-7.
- [12] SP. Lim, QY. Wang, CG. Noble, YL. Chen, H. Dong, B. Zou, F. Yokokawa, S. Nilar, P. Smith, D. Beer, J. Lescar, PY. Shi. Ten years of dengue drug discovery: progress and prospects. *Antiviral. Res.* 100 (2013) 500-519.
- [13] B. Chao, XK. Tong, W. Tang, DW. Li, PL. He, JM. Garcia, LM. Zeng, AH. Gao, L. Yang, J. Li, FJ. Nan, M. Jacobs, R. Altmeyer, JP. Zuo, YH. Hu, Discovery and optimization of 2,4-diaminoquinazoline derivatives as a new class of potent dengue virus inhibitors. *J. Med. Chem.* 55 (2012) 3135-3143.
- [14] B. Zou, WL. Chan, M. Ding, SY. Leong, PY. Shi, PW. Smith, Lead optimization of spiroprazolopyridones: a new and potent class of dengue virus inhibitors. *ACS. Med. Chem. Lett.* 6 (2015) 344-348.
- [15] CS. Kounde, HQ. Yeo, QY. Wang, BK. Yeung, F. Yokokawa, Discovery of 2-oxopiperazine dengue inhibitors by scaffold morphing of a phenotypic high-throughput screening hit. *Bioorg. Med. Chem. Lett.* 27 (2017) 1385-1389.
- [16] F. Benmansour, C. Eydoux, G. Querat, X. Lamballerie, B. Canard, K. Alvarez, JC. Guillemot, K. Barral, Novel 2-phenyl-5-[(E)-2-(thiophen-2-yl)ethenyl]-1,3,4-oxadiazole and 3-phenyl-5-[(E)-2-(thiophen-2-yl)ethenyl]-1,2,4-oxadiazole derivatives as dengue virus inhibitors targeting NS5 polymerase. *Eur. J. Med. Chem.* 109 (2016) 146-156.
- [17] A. Venkatesham, M. Saudi, S. Kaptein, J. Neyts, J. Rozenski, M. Froeyen, A.V. Aerschot. Aminopurine and aminoquinazoline scaffolds for development of potential dengue virus inhibitors. *Eur. J. Med. Chem.* 126 (2017) 101-109.
- [18] AK. Timiri, BN. Sinha, V. Jayaprakash. Progress and prospects on DENV protease inhibitors. *Eur. J. Med. Chem.* 117 (2016) 125-143.
- [19] AJ. Stevens, ME. Gahan, S. Mahalingam, PA. Keller PA. The medicinal chemistry of dengue fever. *J. Med. Chem.* 52 (2009) 7911-7926.
- [20] MA. Behnam, C. Nitsche, V. Boldescu, CD. Klein. The Medicinal Chemistry of Dengue Virus. *J. Med. Chem.* 59 (2016) 5622-5649.
- [21] The data was updated in the Sanofi Pasteur official site: <http://www.sanofipasteur.com/en/>
- [22] K. Monsieura, P. Tapolcsányib, K. Loonesa, G. Neumajerb, J.A. Ridderc, K. Goubitzc, G. Lemièrea, R. Dommissa, P. Mátyus, Is samoquasine A indeed benzo[f]phthalazin-4(3H)-one Unambiguous, straightforward synthesis of benzo[f]phthalazin-4(3H)-one and its regioisomer benzo[f]phthalazin-1(2H)-one. *Tetrahedron.* 63 (2007) 3870-3881.

- [23] W. Mederski, M. Lefort, M. Germann, D. Kux, N-aryl heterocycles via coupling reactions with arylboronic acids. *Tetrahedron*. 55 (1999) 12757-3881.
- [24] H. Lu, Z. Geng, J. Li, D. Zou, Y. Wu, Y. Wu, Metal-Free Reduction of Aromatic Nitro Compounds to Aromatic Amines with B_2pin_2 in Isopropanol. *Org. Lett.* 18 (2016) 2774-2776.
- [25] O. Trott, A.J. Olson, AutoDock Vina: improving the speed and accuracy of docking with a new scoring function, efficient optimization, and multithreading. *J Comput Chem.* 31 (2010) 455-461.

Table, Figure and Scheme Captions

Table 1. SAR study on A ring of phthalazinone core.

Table 2. SAR of substituents on benzyl moiety.

Table 3. SAR study on B ring of phthalazinone core.

Table 4. SAR study of substituents on phenyl moiety.

Table 5: *In Vivo* mice pharmacokinetic properties of compound **14l**

Figure 1. Recently reported DENV inhibitors.

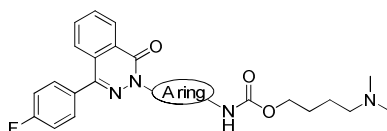
Figure 2. Structure of hit compound **10a**.

Figure 3: The computerized docking modes of **14l** with dengue NS3 protease. A: full view. B: detailed view.

Scheme 1. Synthesis of **10a-10e**.^a

Scheme 2. Synthesis of **11a-11d**.^a

Scheme 3. Synthesis of **14a-14p**.^a

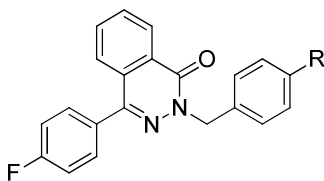


Compd	R	CC ₅₀ (μ M) ^a	IC ₅₀ (μ M) ^b	IC ₉₀ (μ M) ^c	SI ^d
10a		8.51	0.64	4.65	13.3
10b		19.04	0.62	4.27	30.7
10c		48.50	2.83	13.15	17.1
10d		15.16	1.27	5.57	11.9
10e		21.76	1.34	12.62	16.2

^aCC₅₀ is 50% cytotoxicity concentration in Huh 7 cells. ^bIC₅₀ is 50% inhibitory concentration of cytoplasmic DENV-RNA replication. ^cIC₉₀ is 90% inhibitory concentration of cytoplasmic DENV-RNA replication.

^dSelectivity index (SI) = CC₅₀/IC₅₀.

Table 1: SAR study on A ring of phthalazinone core.

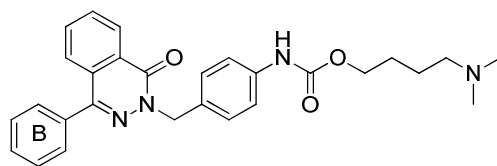


Compd	R	CC ₅₀ (μ M) ^a	IC ₅₀ (μ M) ^b	IC ₉₀ (μ M) ^c	SI ^d
9c	NH ₂	>80	19.96	>80	>4.0
11a		38.20	1.00	8.42	38.2
11b		77.65	1.05	10.65	73.9
11c		46.60	4.35	9.46	10.7
11d		19.5	1.4	>80	14.3

^aCC₅₀ is 50% cytotoxicity concentration in Huh 7 cells. ^bIC₅₀ is 50% inhibitory concentration of cytoplasmic DENV-RNA replication. ^cIC₉₀ is 90% inhibitory concentration of cytoplasmic DENV-RNA replication.

^dSelectivity index (SI) = CC₅₀/IC₅₀.

Table 2: SAR of substituents on benzyl moiety.

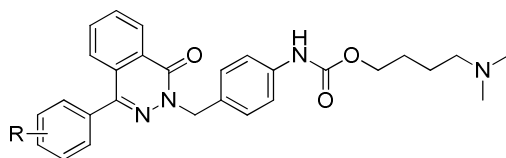


Compd	B ring	CC ₅₀ (μ M) ^a	IC ₅₀ (μ M) ^b	IC ₉₀ (μ M) ^c	SI ^d
14a		65.29	0.60	62.38	108.8
14b		62.67	22.89	40.90	2.7
14c		67.96	6.32	30.22	10.7
14d		55.86	6.53	43.31	8.5
14e		16.04	2.68	6.09	5.99

^aCC₅₀ is 50% cytotoxicity concentration in Huh 7 cells. ^bIC₅₀ is 50% inhibitory concentration of cytoplasmic DENV-RNA replication. ^cIC₉₀ is 90% inhibitory concentration of cytoplasmic DENV-RNA replication.

^dSelectivity index (SI) = CC₅₀/IC₅₀.

Table 3: SAR study on B ring of phthalazinone core.



Compd	R	CC ₅₀ (μ M) ^a	IC ₅₀ (μ M) ^b	IC ₉₀ (μ M) ^c	SI ^d
10b	4-F	19.04	0.62	4.27	30.7
14f	4-OCH ₃	20.34	1.94	5.88	10.5
14g	4-CN	37.00	0.70	7.07	52.8
14h	4-CF ₃	3.36	1.47	6.61	2.3
14i	3-F	37.39	1.51	8.24	24.7
14j	3-OCH ₃	17.63	0.34	1.58	51.8
14k	3-CN	17.18	1.72	5.09	10.0
14l	3-CF ₃	11.59	0.13	1.15	89.2
14m	2-F	52.50	1.32	8.79	39.8
14n	2-OCH ₃	44.75	1.40	5.44	32.0
14o	2-CN	90.71	5.52	12.42	16.4
14p	2-CF ₃	35.72	1.99	3.37	18.0

^aCC₅₀ is 50% cytotoxicity concentration in Huh 7 cells. ^bIC₅₀ is 50% inhibitory concentration of cytoplasmic DENV-RNA replication. ^cIC₉₀ is 90% inhibitory concentration of cytoplasmic DENV-RNA replication.

^dSelectivity index (SI) = CC₅₀/IC₅₀.

Table 4: SAR study of substituents on phenyl moiety.

Dose	CL_{plasma}	V_{ss}	T_{max}	T_{1/2}	C_{max}	AUC_{last}	F
route	(mL/kg/h)	(mL/kg)	(h)	(h)	(ng/mL)	(ng*h/mL)	%
iv	50.0	17137	--	4.33	--	505	--
po	--	--	8	2.91	94.5	883	34.9

^a Experiments were carried out in SD mice (n = 3) Dose: iv, 2.0 mg/kg (5% DMSO, 10% solutol, 10% ethanol, and 75% saline); po, 10.0 mg/kg (5% DMSO, 10% solutol, 10% ethanol, and 75% saline).

Table 5: *In Vivo* mice pharmacokinetic properties of compound **14I**

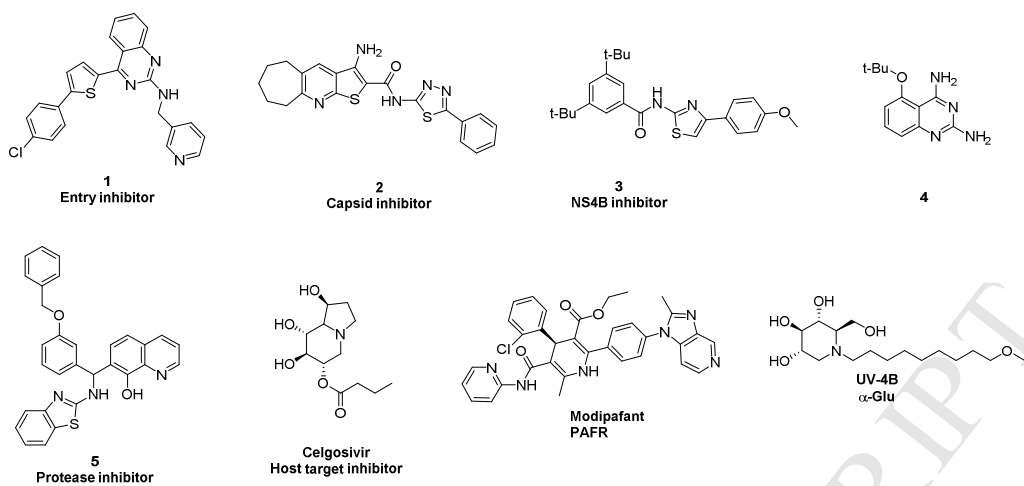
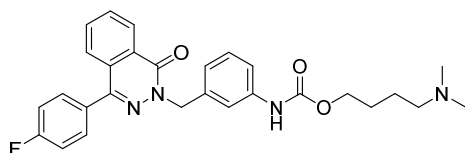


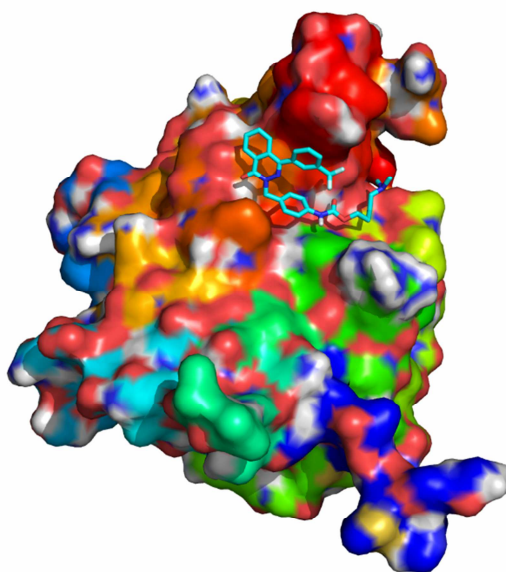
Figure 1: Recently reported DENV inhibitors.



Hit compound 10a

Figure 2: Structure of hit compound 10a.

A:



B:

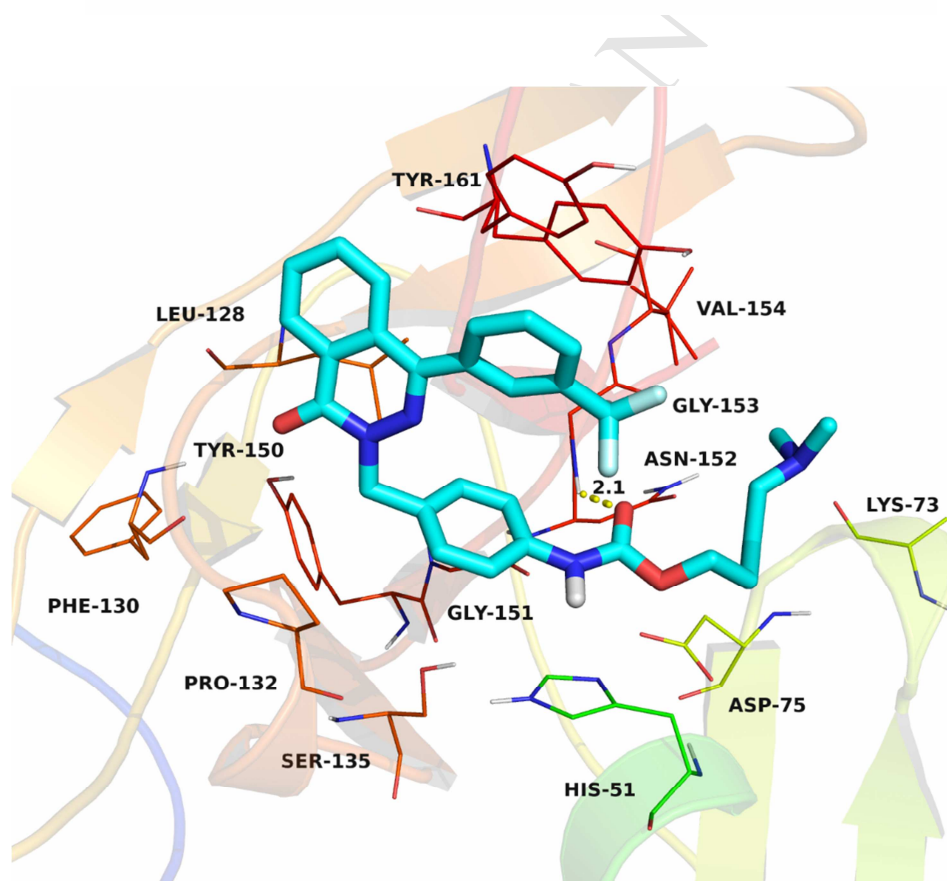
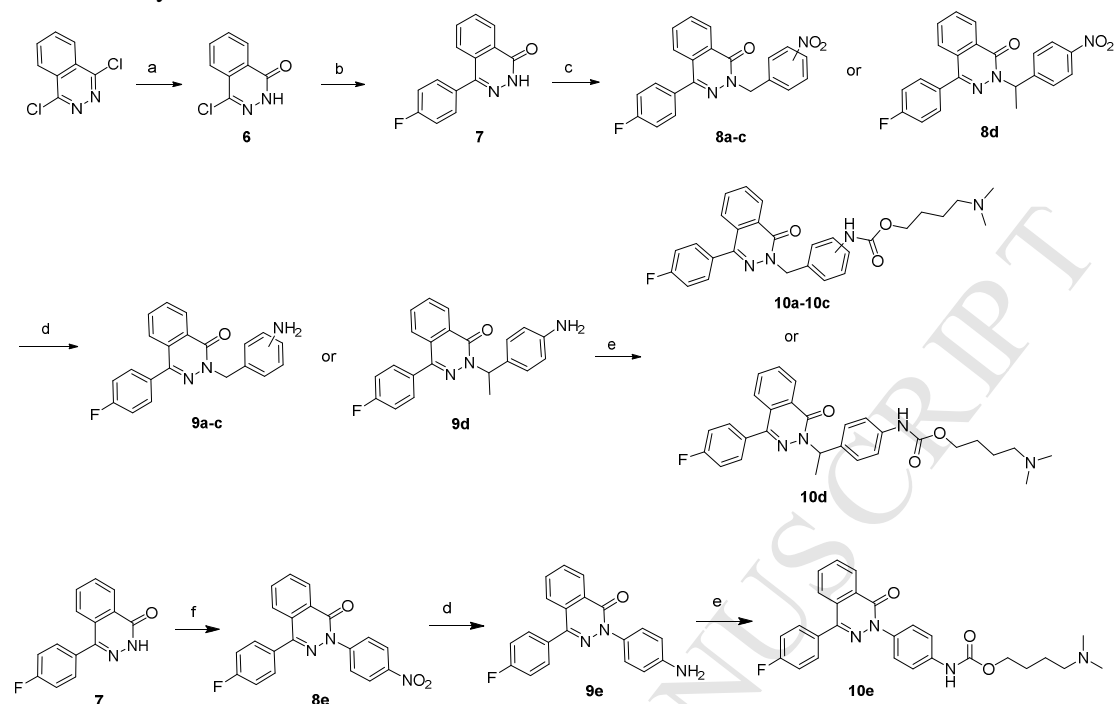
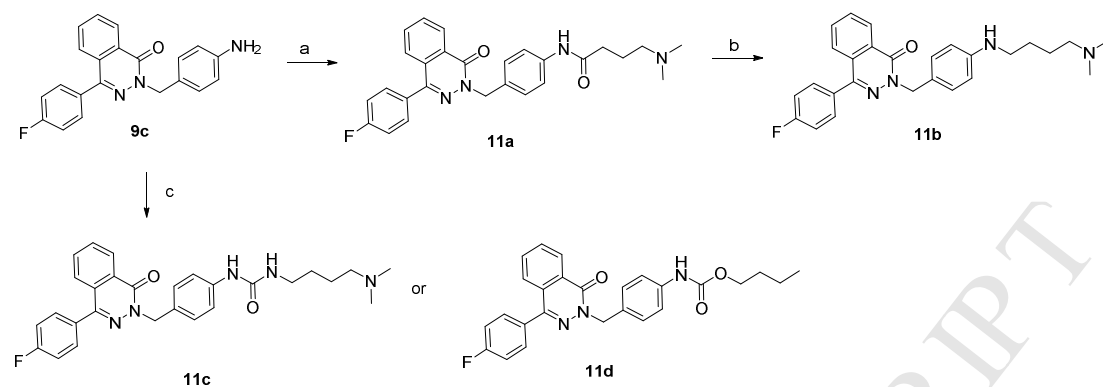


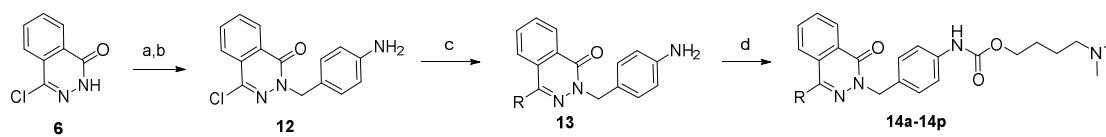
Figure 3: The computerized docking modes of **14l** with dengue NS3 protease. A: full view. B: detailed view.

Scheme 1: Synthesis of 10a-10e.^a

^aReagents and conditions: (a) AcOH, 120 °C, 5h; (b) (4-fluorophenyl)boronic acid, Pd(dppf)₂Cl₂, Cs₂CO₃, dioxane:H₂O = 5:1, 100 °C, overnight; (c) the corresponding bromides, Cs₂CO₃, DMF, 50 °C, overnight; (d) B₂Pin₂, KO^tBu, ⁱPrOH, 110 °C, overnight; (e) (i) triphosgene, Et₃N, anhydrous CH₂Cl₂, 0 °C, 10 min; (ii) 4-(dimethylamino)butan-1-ol, rt, overnight; (f) (4-nitrophenyl)boronic acid, pyridine, Cu(OAc)₂, DMF, rt, overnight.

Scheme 2: Synthesis of 11a-11d.^a

^aReagents and conditions: (a) (i) 4-(dimethylamino)butanoic acid, (COCl)₂, DMF(*cat*), anhydrous CH₂Cl₂, rt, 3h; (ii) 9c, anhydrous THF, rt, overnight; (b) LiAlH₄, anhydrous THF, reflux, 5h; (c) (i) triphosgene, Et₃N, 0 °C, 10 min; (ii) butan-1-ol or N¹,N¹-dimethylbutane-1,4-diamine, rt, overnight.

Scheme 3: Synthesis of 14a-14p.^a

^aReagents and conditions: (a) 1-(bromomethyl)-4-nitrobenzene, Cs₂CO₃, DMF, 50 °C, overnight; (b) B₂Pin₂, KO^tBu, ⁱPrOH, 110 °C, overnight; (c) the corresponding boric acid, Pd(dppf)₂Cl₂, Cs₂CO₃, dioxane:H₂O = 5:1, 100 °C, overnight; (d) (i) triphosgene, Et₃N, CH₂Cl₂, 0 °C, 10 min; (ii) 4-(dimethylamino)butan-1-ol, overnight.